AUTHOR Enas Mangoush, Sufyan Garoushi, Pekka K Vallittu, Lippo Lassila

TITLE Influence of Short Fiber Reinforced Composites on Fracture Resistance of Single-Structure Restorations

YEAR 2020

DOI 10.1922/EJPRD_2075Mangoush10

VERSION Final draft

CITATION Enas Mangoush, Sufyan Garoushi, Pekka K Vallittu, Lippo Lassila: Influence of Short Fiber Reinforced Composites on Fracture Resistance of Single-Structure Restorations. European Journal of Prosthodontics and Restorative Dentistry (2020) 28, 189–198, doi: 10.1922/EJPRD_2075Mangoush10.

Influence of short fibre-reinforced composites on fracture resistance of single-structure restorations

Abstract

Objective: The aim was to determine the load-bearing capacity of anterior crowns prepared using two types of single-structure short fibre-reinforced composites (SFRCs). Furthermore, fracture toughness (FT), flexural strength (FS) and flexural modulus (FM) of tested composites were measured.

Methods: Seven-group of composite crowns were designed for an upper central incisor (n=8/group). Two-group were CAD/CAM fabricated made of Cerasmart 270 and experimental single-structure SFRC blocks. Two-group were 3D-printed made of GC Temp PRINT and Pro3dure GR-17 composites. Two-group were made of conventional light-cured composites (Essentia and Gradia Plus). The last group was single-structure SFRC made of commercial flowable SFRC (everX Flow). Crown restorations were loaded until fracture. Failure-modes were then visually examined. FT, FS and FM were determined for each tested composite (n=8). The data were analysed using analysis of variance ($p=0.05$) followed by Tukey's post-hoc test.

Results: ANOVA revealed that crowns made of experimental SFRC blocks had significantly higher load-bearing capacities (1650 ±230 N) ($p<0.05$) among all the groups tested. Experimental SFRC blocks exhibited the highest FT (2.9 MPa $m^{1/2}$) and FS (245.8 MPa) values ($p<0.05$) among tested composites.

Conclusion: CAD/CAM fabricated restorations made of experimental SFRC blocks demonstrated encouraging performance related to their fracture-behaviour.

Keywords: Fracture behaviour, single-structure restoration, anterior crown, fibre composite, 3D-printing.

Introduction

The practice of metal-free dentistry is growing due to changing medical and aesthetic preferences. Medically, concerns have been reported about adverse effects initiated by metal alloys[1]. Aesthetically, increased attention on a pleasing aesthetic appearance increases the desire for metal-free restorations, even in the molar teeth[2]. All-ceramic crown restorations have been developed to improve aesthetic appearance, which is often better without the underlying metal. However, all-ceramic restorations have some disadvantages. They are brittle and expensive, require more tooth reduction, require a complicated bonding procedure, and might cause abrasive wear of antagonist dentition[2,3]. A preferable alterative to all-ceramic crown restorations is achieved with indirect composite restorations. Different from ceramics, composites are relatively cheap, easy to construct, and promote less wear of the opposing dentition[4-6]. Many studies have been focused on the clinical performance of composite crown restorations made by either the manual build-up technique or computer-aided design computer-aided manufacturing (CAD/CAM) technique[7-9]. The major cause for failure in all studies was a catastrophic fracture, implying that the toughness of composite crown restorations is a critical property for achieving a good clinical result. The brittleness of composites is caused by a low resistance to crack extension and in most cases these materials fail due to unstable crack propagation[10,11].

Load-bearing capacity and deformation of restorative composites have usually been assessed by measuring the basic material parameters of fracture toughness and flexural strength and modulus[10]. Fracture toughness is a mechanical characteristic that explains the resistance of brittle materials to the crack growth under functional load. Hence, it describes destruction tolerance of the material and can be seen as a measure of fatigue resistance[10]. Many authors in the literature have stated that materials which have high fracture toughness has the ability to

better resist crack propagation and thus, the property of fracture toughness has become an important criteria in a dental composite's durability[11-13].

Research has been conducted to find ways of improving the toughness and durability of final large composite restorations. Until this time, composites reinforced with short randomly oriented glass fibres (SFRCs) are interesting materials because of their improved fracture toughness and ability to arrest crack propagation[11,14,15]. Earlier, the application of SFRC for single-structure restorations has been discussed[16,17], and the multi-directional fibre orientation of SFRC exhibited an isotropic reinforcing effect. In other words, the strength of the SFRC is not related to the direction of the fracture force[18]. Nevertheless, SFRC has not been well analysed in view of its application as a restorative material for single-structure restorations.

Thus, it was hypothesised that single-structure SFRC restorations, i.e. either made of experimental SFRC CAD/CAM block or manually built-up commercial SFRC, would have sufficient strength for anterior single-structure restorations. Thus, the purpose of the present study was to determine the static load-bearing capacity of anterior single-structure SFRC restorations under *in vitro* loading conditions. The comparison was defined using recently available major restorative composite materials, including flowable (direct/indirect) particulate filler composites (PFCs), CAD/CAM composite block and 3D-printed composites. Furthermore, it was hypothesized that, fracture behaviour of single-structure restorations can be influenced by fracture toughness values of composite materials.

Materials and methods

The materials used in this study are listed in Table 1.

Crown fabrication

An experimental abutment (model) for a crown restoration of the maxillary central incisor was cut from Cobalt Chromium blank (Sintermetall, Zirkonzahn GmbH) using a CAD/CAM device (5-TEC, Zirkonzahn GmbH). Next, the abutment was sintered in a furnace (Zirkonofen 700/UV, Zirkonzahn GmbH) according to the product instructions. After that, the metal abutment was embedded in a plastic tube with acrylic resin except for 2 mm of the cervical area (Figure 1). A photo-impression was taken of the abutment using another dental CAD/CAM device (CEREC, Sirona Dental Systems Inc). A single-structure crown restoration was designed, and a flat surface was created at the incisor edge in order to adapt the loading cell during the fracture test.

A total of 56 single-structure composite crown restorations were allocated to seven groups (n=8/group) according to the fabrication methods. Two groups were CAD/CAM fabricated (CEREC) made of Cerasmart 270 and experimental SFRC blocks. Two groups were 3D-printed made of GC Temp PRINT and Pro3dure GR-17 composites by using a digital light processing printer (Asiga Max UV, Asiga). Last three groups were manually made by build-up of conventional PFC (Essentia and Gradia Plus) and commercial SFRC (everX Flow) composites. For these groups, a transparent template matrix (Memosil 2, Heraeus Kulzer GmbH) of an ideally contoured crown was used to aid standardized crown restorations. The composite pastes were packed into the space created between the index and the abutment, followed by light curing from all directions using a hand-light curing unit (Elipar TM S10, 3M ESPE) for 40 s per increment (wavelength of the light was between 430 and 480 nm and light intensity was 1600 mW/cm^2). The light source was placed in close contact (1-2 mm) with the composite

surface. Gradia Plus restorations were further polymerised in a light-curing oven (Targis Power, Ivoclar Vivadent) according to the manufacturers' instructions.

Before cementation, the inner surface of all CAD/CAM fabricated and 3D-printed restorations was acid etched by hydroflouric acid (Pulpdent Corp) for 60 s followed by washing, air-drying and application of primer (G-Multi Primer, GC). The restorations were then cemented to the sandblasted metal abutment using a metal primer (Metal Primer Z, GC) and luting cement (G-CEM linkForce, GC). Luting cement was not used with manually made restorations and the crowns were tightly fixed solely by resin. Prior to testing, all crown restorations were polished and stored dry for 48 h at 37°C.

Fracture load test

A static load was applied to the crown restorations with a universal testing machine (Lloyd model LRX, Lloyd Instruments Ltd) at a speed of 1 mm/min. The acrylic block containing the metal abutment and restoration was tightly fixed to the inclined metal base to provide a 45-degree angle between the palatal surface of the incisal edge and the loading tip (Figure 1). In order to load onto the flat incisor surface under the same conditions for all tested crown restorations, sheets of aluminium foils were placed above the flat surface. The loading event was registered until restoration fracture (final drop in the load-deflection curve) and the fracture pattern for each specimen was visually analysed by two investigators.

Mechanical tests

Single-edge-notched-beam specimens ($2.5 \times 5 \times 25$ mm^3) according to adapted ISO 20795-2 standard methods were prepared to determine the fracture toughness (FT). An accurately designed slot was fabricated centrally in the specimen extending until its mid-height, which enabled the crack length (x) to be half of specimen's height. The specimens from each group (n=8) were stored dry at 37 °C for 48 h before testing. The specimens were tested in three-point bending mode, in a universal material testing machine (Lloyd Instruments) at a crosshead speed

of 1 mm/min and data were recorded using PC software (Nexygen Lloyd Instruments). The contact point (compression side) of the loading tip to the specimen was at the middle and parallel to the crack present on the tension side (lower part).

The fracture toughness (FT) was calculated using the equation:

$$K_{max} = \left[\frac{P \cdot L}{B} \cdot W^{3/2}\right] \cdot f(x)$$

where:

f is a geometrical function dependent on x:

$$f(x) = 3x^{1/2}\left[1{,}99 - x(1-x)(2{,}15 - 3{,}93x + 2{,}7x^2\right] \Big/ \left[2(1+2x)(1-x)^{3/2}\right]$$

Here P is the maximum load in kilonewtons (kN), L is the span length (2 cm), B is the specimen thickness in centimeters (cm), W is the specimen width (depth) in cm, x is a geometrical function dependent on a/W and a is the crack length in cm.

Three-point bending test specimens (2 x 2 x 25 mm^3) were made from each tested composite. Bar-shaped specimens from each material (n=8) were stored dry at 37 °C for 48 h before testing. The three-point bending test was conducted according to the ISO 4049 (test span: 20 mm, cross-head speed: 1 mm/min, indenter: 2 mm diameter). All specimens were loaded in a universal testing machine and the load-deflection curves were recorded with PC-computer software. Flexural strength (σ_f) and flexural modulus (E_f) were calculated from the following formula:

$\sigma_f = 3F_mI /(2bh^2)$

$E_f = SI^3 /(4bh^3)$

Where Fm is the applied load (N) at the highest point of the load-deflection curve, I is the span length (20 mm), b is the width of the test specimens and h is the thickness of the test specimens.

S is the stiffness (N/m) S=F/d and d is the deflection corresponding to load F at a point in the straight-line portion of the trace.

For CAD/CAM materials, bar-shaped specimens to measure the fracture toughness (1.8 × 3.6 × 18 mm^3) and flexural properties (1.2 × 4 × 14 mm^3) according to ISO 6872:2008 were verified for the three-point bending test. The bar-shaped specimens were prepared using a low-speed diamond saw (Struers). All specimens were wet ground and polished by #4000-grit silicon carbide papers at 300 rpm under water cooling using an automatic grinding machine (Rotopol-1; Struers). After polishing, all specimens were stored and tested as mentioned earlier.

Microscopic analysis

Scanning electron microscopy (SEM, LEO) provided the characterisation of the microstructure of the investigated materials. Polished specimens (n=2) from each material were stored in a desiccator for one day. Then, they were coated with a gold layer using a sputter coater in a vacuum evaporator (BAL-TEC SCD 050 Sputter Coater) before the SEM examination. SEM observations were carried out at an operating voltage of 8 kV and working distance of 13 mm.

Statistical analysis

The data were analyzed using SPSS version 23 (SPSS, IBM Corp.) using analysis of variance (ANOVA) at the $p<0.05$ significance level followed by a Tukey HSD post hoc test to determine the differences between the groups. Pearson's correlation coefficient was calculated to examine the relationship between the investigated mechanical properties of the materials and the fracture load of the crown restorations.

Results

The mean (± SD) fracture load values of the crown restorations are given in Figure 2. ANOVA revealed that crown restorations made of experimental SFRC blocks had significantly higher load-bearing capacities (1650 ±230 N) ($p<0.05$) among all the groups tested. No statistically significant differences were found in the load-bearing capacities between crowns made by 3D-printing technology and those manually made of plain PFCs (Figure 2). ANOVA showed that crowns made of flowable SFRC (everX Flow) had a statistically significantly higher load-bearing capacity (1310 ±397 N) than restorations made of conventional PFCs ($p<0.05$). No statistically significant differences ($p>0.05$) were found between restorations made of SFRC (everX Flow) and those made of CAD/CAM composite block (Cerasmart 270).

Fracture toughness, flexural strength and flexural modulus mean values for tested composite materials with standard deviations (SD) are summarised in Figures 3-5. Experimental SFRC blocks exhibited the highest FS (245.8 MPa) values ($p<0.05$) and FT (2.9 MPa $m^{1/2}$) which was not significantly different ($p>0.05$) from everX Flow (2.8 MPa $m^{1/2}$).

Experimental SFRC blocks presented also the highest FM (14.7 GPa) which was not significantly different ($p>0.05$) from PFC (Essentia, 12.9 GPa). Visual inspection revealed splitting fracture pattern for all crown restorations.

The regression analysis (Figure 6) demonstrated a relatively linear relationship between fracture toughness values and load-bearing capacity (R^2 =0.7437, $p<0.05$) and not for flexural strength (R^2 =0.4653) and flexural modulus (R^2 =0.2699) values.

SEM analysis presented the microstructure of each tested material with different fibres and particulate filler size and shape in the polymer matrix (Figure 7). This proposed an explanation for the varying performance between the tested materials.

Discussion

In the present study, the experimental SFRC CAD/CAM block and commercial flowable SFRC (everX Flow) consisted of the same quantity of discontinuous short glass fibres with a diameter of 6 µm and length in range of 200-300 µm[20]. The SFRC has earlier been reported to reveal high load-bearing capacity and fracture toughness[11,15,19]. Thus, we hypothesised that SFRC could withstand the forces required for anterior crown restorations made either of manually veneered SFRC or experimental SFRC CAD/CAM blocks.

The results of the loading test support our hypothesis because SFRC restorations presented a significant improvement in load-bearing capacity and fracture toughness when compared with other composite materials (Figure 2). The reinforcing effect of the glass fibre is based on the stress transfer from the polymer matrix to the glass fibre, along with the behaviour of the crack stopper within individual pieces of glass fibre. Consequently, single-structure SFRC restorations showed higher fracture behaviour than other particulate-reinforced composites that have recently become available (CAD/CAM, 3D-printed and manually veneered groups). Our results are in line with that of Nagata *et al*., and Garoushi *et al*., who presented a high fracture resistance of anterior composite restorations containing short discontinuous glass fibres[17,20].

Interestingly, the fracture load of the experimental SFRC CAD/CAM restorations was significantly higher than that of the commercial veneered SFRC (everX Flow), although the glass fibre content was similar (Table 1). This could be attributed to the difference in particulate filler inclusion, which resulted in improved mechanical properties of experimental SFRC CAD/CAM composite (Figure 7). Another possible reason, experimental SFRC CAD/CAM blocks were well polymerised with photo-curing and heat-curing, while the veneered SFRC was polymerised using hand photo-curing without heat-curing. Consequently, the experimental SFRC CAD/CAM blocks had better mechanical properties than the veneered SFRC in the present study.

Although 3D-printed composites have low particulate filler content and thus intended for interim clinical use, no differences were found in the load-bearing capacities between crowns made by 3D-printing technology and those manually made of plain PFCs (Figure 2). Previous studies with composites have shown that critical strain energy release rate can be improved with the inclusion of a certain filler-volume fraction, but further than the critical filler content, the energy release rate reduces[21,22]. Therefore, there may exist a most favourable filler-volume fraction and filler particle size that could create an optimal critical stress-intensity factor and this might justify why there was no significant difference for most of the tested mechanical properties among 3D-printed composites (with low filler content) and those high filled PFCs (Figure 7).

Visible light with adequate intensity and wavelength and for a sufficient curing time are critical for adequate polymerisation of photo-polymerised composites[23].

Generally, our results are in agreement with previous *in vitro* studies, which showed that additional post-curing resulted in increased mechanical properties of composite materials by improving the degree of monomer conversion[16,24]. Though, certain differences could also be justified as a result of differences in polymer matrices and the filler content of the materials we used.

In the present study, the experimental SFRC blocks exhibited a significantly higher fracture toughness (2.9 MPa $m^{1/2}$) and high flexural strength and modulus values than other tested composites (Figure 3). And this is in accordance with previous studies, which showed superior fracture toughness of flowable SFRC than PFC composites[15,19,25].

For restorative material evaluation, a number of mechanical properties could be considered. The mechanical tests used in this study followed the well-established and widely recognised test method described in the ISO standard[26]. Fracture toughness and flexural properties were selected as they describe the responses of materials to loading and crack propagation. The

geometrical parameters of the 3-point bending test specimens for restorative composites (ISO 4049:2009) and ceramics (ISO 6872:2008) are not identical. Owing to the size limitation of the CAD/CAM block, the geometrical parameters for ceramics were chosen for CAD/CAM groups. The flexural properties achieved from the two standard tests were reported not identical, but provided similar findings[27-29].

In line with previous studies[11,15], a positive relationship between fracture toughness values and load-bearing capacity results was noticed in this study (Figure 6). As explained previously, fracture toughness describes damage tolerance and can be designed as a measure of crack resistance of the material, which predicts fatigue performance. As modern composite materials are brittle, they have a lack of toughness, not strength[12].

According to visual fracture pattern analysis of the of the crown restorations, only typical splitting failure was found among the materials used. In the present study, the fracture loads were equally applied to the incisor edge area, which is considered to be the most vital area of the maxillary central incisor from a mechanical perspective[17]. The cracks in all crown restorations initiated at a similar point, near the flat surface of the incisor edge area. This result may indicate that the aluminium foils that were placed between the restorations and the load cell (Figure 1) offered constant loading condition.

The use of crowns prepared and tested on a metal model could be considered limitation of this study. A metal (cobalt chromium) model was used because it aids standardisation of the crown abutment and the crown shape, allowing the effect of the material type to be the only variable factor. Sakoguchi *et al*., studied the influence of model (abutment) materials on the fracture behaviour of composite crowns for premolars[30]. They showed that load-bearing values of composite crowns mounted on metal model were significantly lower than those mounted on resin models, despite the composite crown material used. According to them, the load-bearing

capacity of crowns fabricated with brittle materials was affected by two factors: bonding strength to model and matching of flexural modulus between crown and model materials.

An oblique load (45° to the long axis of the tooth) was applied to the tested restorations, which seems to be the worst-case scenario in relation to the load-bearing capacity of anterior crowns[31]. Another limitation of this investigation is that static load to failure testing was used to determine maximal load-bearing capacity instead of applying dynamic loading cycles. Teeth and dental restorations are usually subjected to low and cyclic forces instead of being impactive in nature. However, owing to the linear relationship between static and fatigue loading, the static test setup also gives valuable information regarding the fracture behaviour and load-bearing capacity[32]. Although the load-bearing value is typically much higher than functional biting loads, it is still a valid method for comparing different restorative materials.[33] Given the stated limitations, the proposed methodology should require future testing with cyclic loading. It should be taken into account that commercial micrometer scale SFRC (everX Flow) is instructed to be used as bulk base or core foundation and should not be used as final restoration. Although, microfibers filler loading were not worsening the wear neither the gloss of the flowable SFRC.[34,35] Therefore, surface and aesthetic properties such as wear, gloss and color stability of the experimental SFRC CAD/CAM blocks should also be evaluated in the future.

Conclusion

Within the limitation of this study, single-structure CAD/CAM fabricated restorations made of experimental SFRC blocks displayed promising performance related to fracture-behaviour.

References

1. Wataha JC. Biocompatibility of dental casting alloys: a review. J Prosthet Dent 2000; **83**:223–234.

2. Li RW, Chow TW, Matinlinna JP. Ceramic dental biomaterials and CAD/CAM technology: state of the art. J Prosthodont Res 2014; **58**:208–216.

3. Kassem AS, Atta O, El-Mowafy O. Fatigue resistance and microleakage of CAD/CAM ceramic and composite molar crowns. J Prosthodont 2012; **21**:28–32.

4. Awada A, Nathanson D. Mechanical properties of resin-ceramic CAD/CAM restorative materials. J Prosthet Dent 2015; **114**:587–593.

5. Attia A, Abdelaziz KM, Freitag S, Kern M. Fracture load of composite resin and feldspathic all-ceramic CAD/CAM crowns. J Prosthet Dent 2006; **95**:117-123.

6. Ghazal M, Albashaireh ZS, Kern M. Wear resistance of nanofilled composite resin and feldspathic ceramic artificial teeth. J Prosthet Dent 2008; **100**:441-448.

7. Rammelsberg P, Spiegl K, Eickemeyer G, Schmitter M. Clinical performance of metal-free polymer crowns after 3 years in service. J Dent 2005; **33**:517–523.

8. Vanoorbeek S, Vandamme K, Lijnen I, Naert I. Computer aided designed/computer-assisted manufactured composite resin versus ceramic single-tooth restorations: a 3-year clinical study. Int J Prosthodont 2010; **23**:223–230.

9. Ohlmann B, Bermejo JL, Rammelsberg P, Schmitter M, Zenthöfer A, Stober T. Comparison of incidence of complications and aesthetic performance for posterior metal-free polymer crowns and metal-ceramic crowns: results from a randomized clinical trial. J Dent 2014; **42**:671–676.

10. Craig RG (Ed.) 1997. Restorative dental materials 10, Mosby Publishing Co, St. Louis, MO.

11. Lassila L, Keulemans F, Säilynoja E, Vallittu PK, Garoushi S. Mechanical properties and fracture behavior of flowable fiber reinforced composite restorations. Dent Mater 2018; **34**:598–606.

12. Kim KH, Okuno O. Microfracture behaviour of composite resins containing irregular-shaped fillers. J Oral Rehabil 2002; **29**:1153-1159.

13. Ruddell DE, Maloney MM, Thompson JY. Effect of novel filler particles on the mechanical and wear properties of dental composites. Dent Mater 2002; **18**:72-80.

14. Garoushi S, Gargoum A, Vallittu PK, Lassila L. Short fiber-reinforced composite restorations: A review of the current literature. J Investig Clin Dent 2018; **9**:e12330.

15. Lassila L, Säilynoja E, Prinssi R, Vallittu PK, Garoushi S. Fracture behavior of Bi-structure fiber-reinforced composite restorations. J Mech Behav Biomed Mater 2020; **101**:103444.

16. Garoushi S, Vallittu PK, Lassila LV. Fracture resistance of short, randomly oriented, glass fiber-reinforced composite premolar crowns. Acta Biomater 2007; **3**:779–784.

17. Nagata K, Garoushi SK, Vallittu PK, Wakabayashi N, Takahashi H, Lassila LVJ. Fracture behavior of single-structure fiber-reinforced composite restorations. Acta Biomater Odontol Scand 2016; **2**:118–124.

18. Lästumäki TM, Lassila LV, Vallittu PK. Flexural properties of the bulk fiber-reinforced composite DC-Tell used in fixed partial dentures. Int J Prosthodont 2001; **14**:22-26.

19. Lassila L, Säilynoja E, Prinssi R, Vallittu P, Garoushi S. Characterization of a new fiber-reinforced flowable composite. Odontology 2019; **107**:342–352.

20. Garoushi S, Vallittu PK, Lassila LV. Direct restoration of severely damaged incisors using short fiber-reinforced composite resin. J Dent 2007; **35**:731–736.

21. Rodrigues Jr SA, Scherrer SS, Ferracane JL, Della Bona A. Microstructural characterization and fracture behavior of a microhybrid and a nanofill composite. Dent Mater 2008; **24**:1281–1288.

22. Masouras K, Silikas N, Watts DC. Correlation of filler content and elastic properties of resin-composites. Dent Mater 2008; **24**:932–939.

23. Garoushi S, Vallittu P, Shinya A, Lassila L. Influence of increment thickness on light transmission, degree of conversion and micro hardness of bulk fill composites. Odontology 2016; **104**:291–297.

24. Loza-Herrero MA, Rueggeberg FA, Caughman WF, Schuster GS, Lefebvre CA, Gardner FM. Effect of heating delay on conversion and strength of a post-cured resin composite. J Dent Res 1998; **77**:426–431.

25. Garoushi S, Vallittu P, Lassila L. Mechanical properties and radiopacity of flowable fiber-reinforced composite. Dent Mater J 2019; **38**:196–202.

26. Ilie N, Hilton TJ, Heintze SD, *et al*. Academy of Dental Materials guidance-Resin composites: Part I-Mechanical properties. Dent Mater 2017; **33**:880–894.

27. Takahashi H, Nakano F, Tonami K, *et al*. Effect of the test methods on flexural properties of dental restorative materials. J J Dent Mater 1999; **18**:395-400.

28. Lauvahutanon S, Takahashi H, Shiozawa M, *et al*. Mechanical properties of composite resin blocks for CAD/CAM. Dent Mater J 2014; **33**:705–710.

29. Harada A, Nakamura K, Kanno T, *et al*. Fracture resistance of computer-aided design/computer-aided manufacturing-generated composite resin-based molar crowns. Eur J Oral Sci 2015; **123**:122–129.

30. Sakoguchi K, Minami H, Suzuki S, Tanaka T. Evaluation of fracture resistance of indirect composite resin crowns by cyclic impact test: influence of crown and abutment materials. Dent Mater J 2013; **32**:433–440.

31. Wandscher VF, Bergoli CD, Limberger IF, Ardenghi TM, Valandro LF. Preliminary results of the survival and fracture load of roots restored with intracanal posts: weakened vs nonweakened roots. Oper Dent 2014; **39**:541–555.

32. Garoushi S, Lassila LVJ, Tezvergil A, Vallittu PK. Static and fatigue compression test for particulate filler composite resin with fiber-reinforced composite substructure. Dent Mater 2007; **23**:17–23.

33. Özcan M, Höhn J, Araujo GM, Moura DM, Rodrigo OA, SOUZA RO. Influence of testing parameters on the load-bearing capacity of prosthetic materials used for fixed dental prosthesis: A systematic review. Braz Dent Sci 2018; **21**:470-490.

34. Lassila L, Keulemans F, Vallittu PK, Garoushi S. Characterization of restorative short-fiber reinforced dental composites. Dent Mater J 2020 in press.

35. Lassila L, Säilynoja E, Prinssi R, Vallittu PK, Garoushi S. The effect of polishing protocol on surface gloss of different restorative resin composites. Biomater Investig Dent 2020; **7**:1-8.

Manufacturer Details

- Sintermetall, Zirkonzahn GmbH, Gais BZ, Italy
- 5-TEC, Zirkonzahn GmbH, Gais BZ, Italy
- Zirkonofen 700/UV, Zirkonzahn GmbH, Gais BZ, Italy
- CEREC, Sirona Dental Systems Inc., Long Island City, NY
- Asiga Max UV, Asiga, Sydney, Australia
- Memosil 2, Heraeus Kulzer GmbH, Hanau, Germany
- Elipar TM S10, 3M ESPE, Seefeld, Germany
- Targis Power, Ivoclar Vivadent AG, Liechtenstein
- Pulpdent Corp, Watertown, USA
- G-Multi Primer, GC, Tokyo, Japan
- Metal Primer Z, GC, Tokyo, Japan
- G-CEM linkForce, GC, Tokyo, Japan
- Lloyd model LRX, Lloyd Instruments Ltd, Fareham, UK
- Nexygen Lloyd Instruments, Fareham, UK
- Struers, Glasgow, Scotland
- Rotopol-1; Struers, Copenhagen, Denmark
- SEM, LEO, Oberkochen, Germany
- BAL-TEC SCD 050 Sputter Coater, Balzers, Liechtenstein
- SPSS, IBM Corp. NY
- Gradia Plus, GC, Tokyo, Japan
- CERASMART 270, GC, Tokyo, Japan
- Essentia Universal, GC, Tokyo, Japan
- TEMP PRINT medium, GC, Tokyo, Japan
- GR-17 temporary, Pro3dure Medical, Iserlohn, Germany
- everX Flow, GC, Tokyo, Japan

Acknowledgments

Testing materials were provided by the manufacturing companies, which is greatly appreciated.

Table 1. The composite materials used in the study

Material (type)	Manufacturer	Composition
Gradia Plus (Lab)	GC Corp,	UDMA, dimethacrylate, inorganic fillers (71 wt%), Prepolymerized fillers (6 wt%)
CERASMART 270 (CAD/CAM)	GC Corp,	Bis-MEPP, UDMA, DMA, Silica (20 nm), barium glass (300 nm) 71 wt%
Essentia Universal (Chair-side)	GC Corp,	UDMA, BisEMA, BisGMA, TEGDMA, Bis-MEPP, Prepolymerized silica and barium glass 81 wt%
TEMP PRINT medium (3D)	GC Corp,	UDMA, dimethacrylate, inorganic silica fillers < 25 wt%
GR-17 temporary (3D)	Pro3dure Medical,	Bismethacrylate and dimethacrylate monomers, silicon dioxide < 50wt%
SFRC Block (CAD/CAM)	Experimental	UDMA, TEGDMA, Short glass fiber (200-300 µm & Ø7 µm), Barium glass 77 wt%
everX Flow (Chair-side)	GC Corp,	Bis-EMA, TEGDMA, UDMA, Short glass fiber (200-300 µm & Ø7 µm), Barium glass 70 wt%

Bis-GMA, bisphenol-A-glycidyl dimethacrylate; TEGDMA, triethylene glycol dimethacrylate; UDMA, urethane dimethacrylate; Bis-MEPP, Bis (p-methacryloxy (ethoxy)1-2 phenyl)-propane; Bis-EMA, Ethoxylated bisphenol-A-dimethacrylate; wt%, weight percentage; vol%, volume percentage.

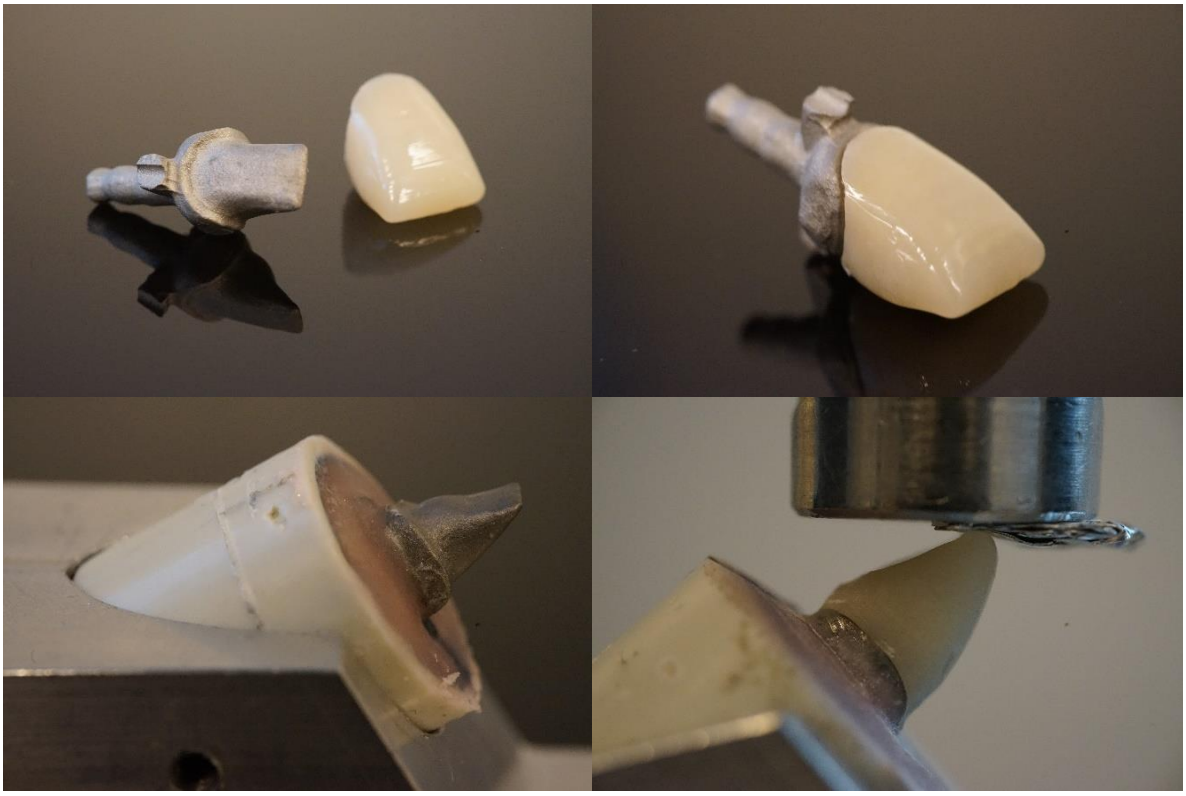

Figure 1. A photograph showing test specimen and the static load test setup.

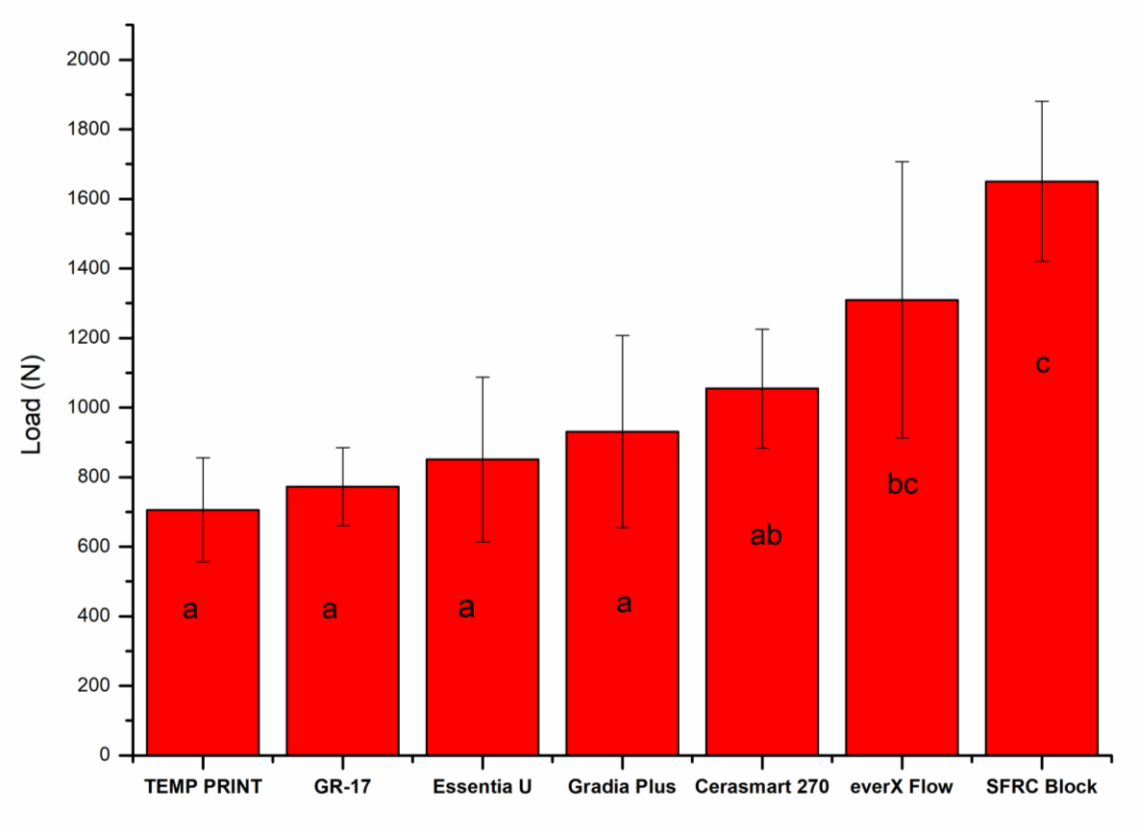

Figure 2. Mean values of load-bearing capacity (N) and standard deviation (SD) of tested restorations. The same letters inside the bars represent non-statistically significant differences ($p>0.05$) among the materials.

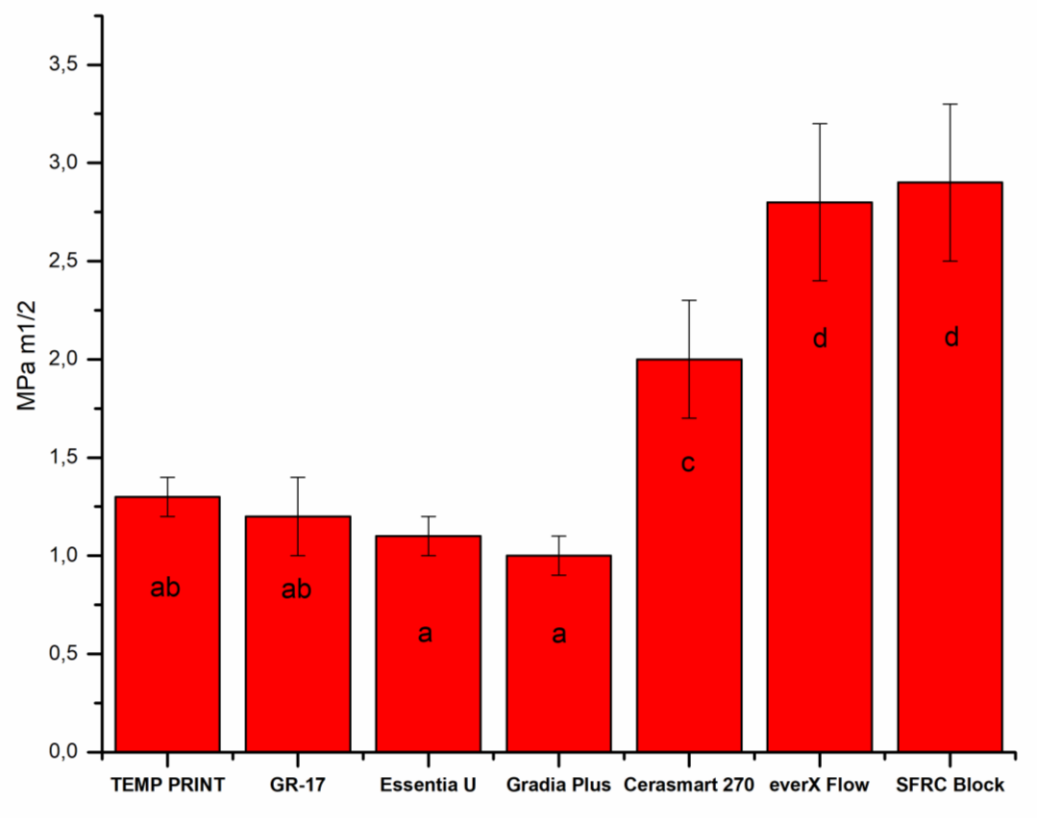

Figure 3. Bar graph illustrating means of fracture toughness (K_{IC}) and standard deviations (SD) of investigated composites. The same letters inside the bars represent non-statistically significant differences ($p>0.05$) among the materials.

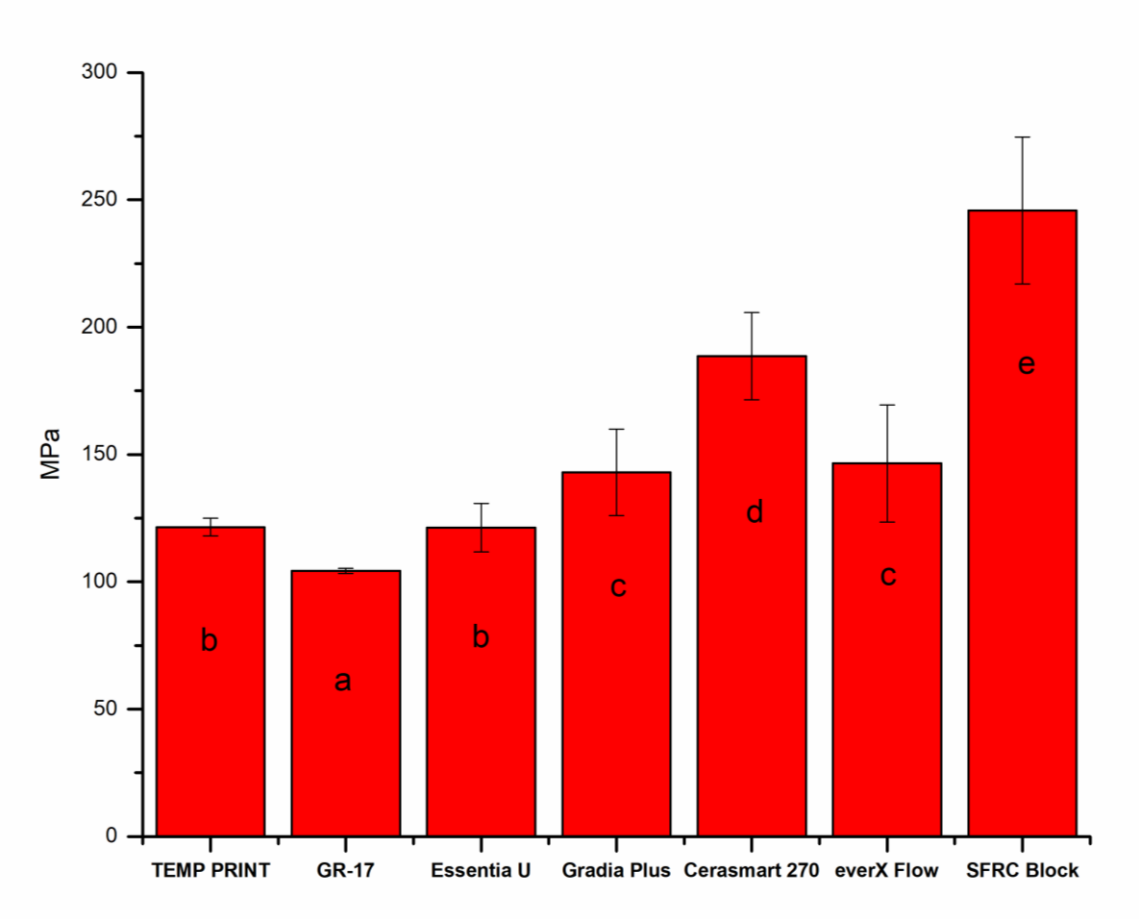

Figure 4. Bar graph illustrating means flexural strength (MPa) and standard deviations (SD) of investigated composites. The same letters inside the bars represent non-statistically significant differences ($p>0.05$) among the materials.

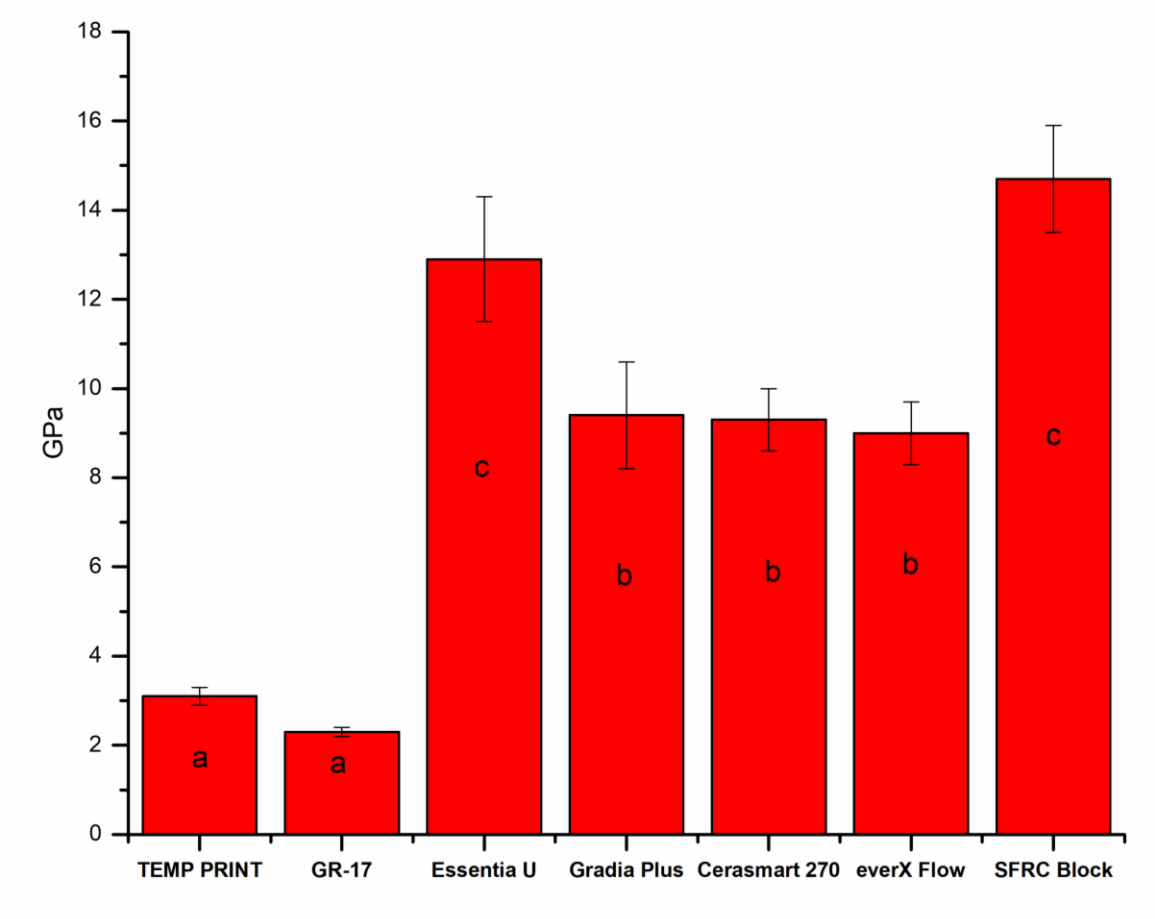

Figure 5. Bar graph illustrating means flexural modulus (GPa) and standard deviations (SD) of investigated composites. The same letters inside the bars represent non-statistically significant differences ($p>0.05$) among the materials.

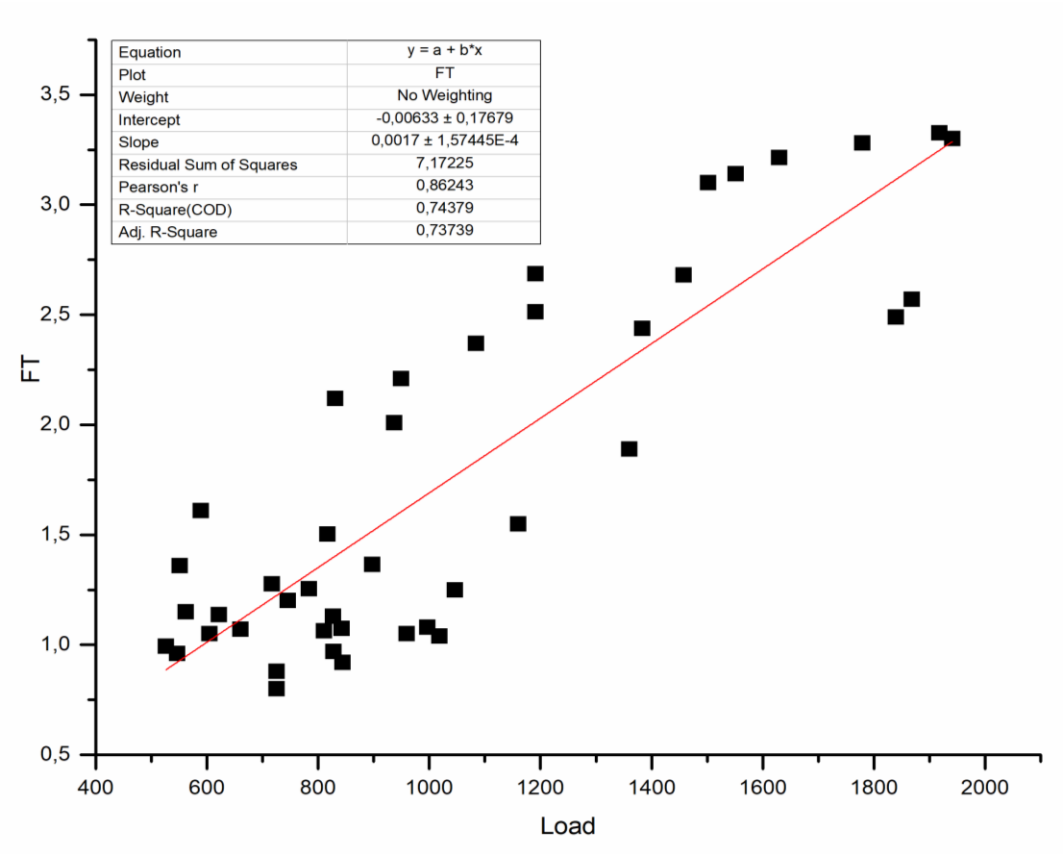

Figure 6. Linear regression between measured fracture toughness (MPa $m^{1/2}$) of the materials and the load-bearing capacities (N) of tested specimens.

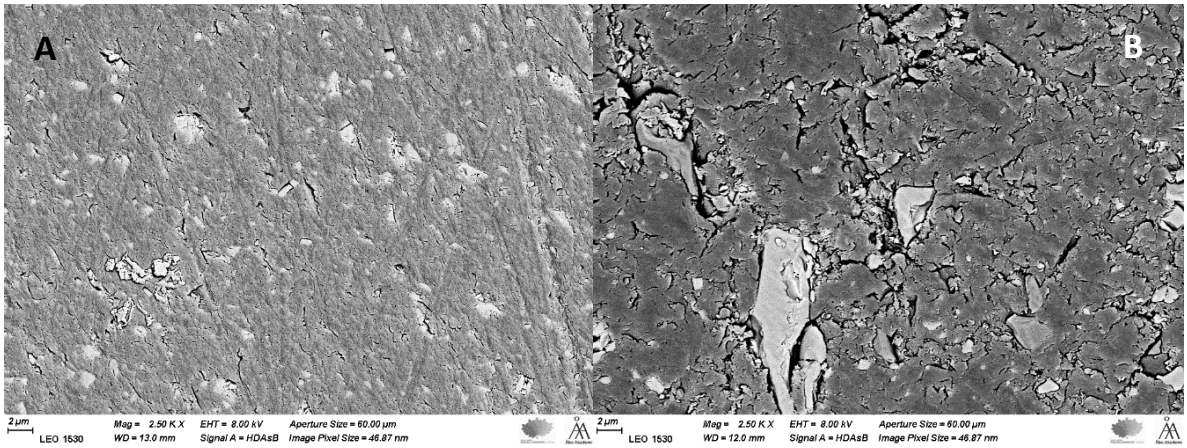
A
2 µm
LEO 1530
Mag = 2.50 K X
WD = 13.0 mm
EHT = 8.00 kV
Signal A = HDAsB
Aperture Size = 60.00 µm
Image Pixel Size = 46.87 nm

B
2 µm
LEO 1530
Mag = 2.50 K X
WD = 12.0 mm
EHT = 8.00 kV
Signal A = HDAsB
Aperture Size = 60.00 µm
Image Pixel Size = 46.87 nm

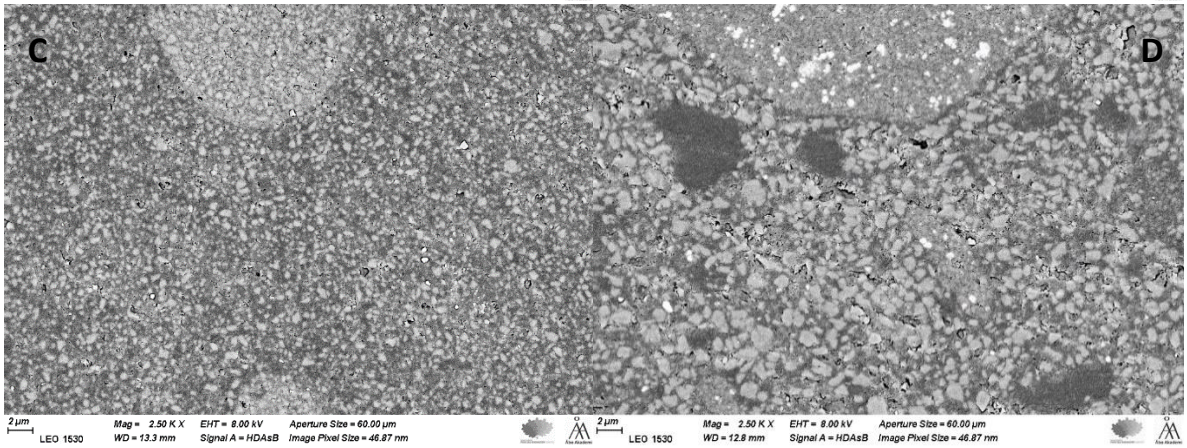
C
2 µm
LEO 1530
Mag = 2.50 K X
WD = 13.3 mm
EHT = 8.00 kV
Signal A = HDAsB
Aperture Size = 60.00 µm
Image Pixel Size = 46.87 nm

D
2 µm
LEO 1530
Mag = 2.50 K X
WD = 12.8 mm
EHT = 8.00 kV
Signal A = HDAsB
Aperture Size = 60.00 µm
Image Pixel Size = 46.87 nm

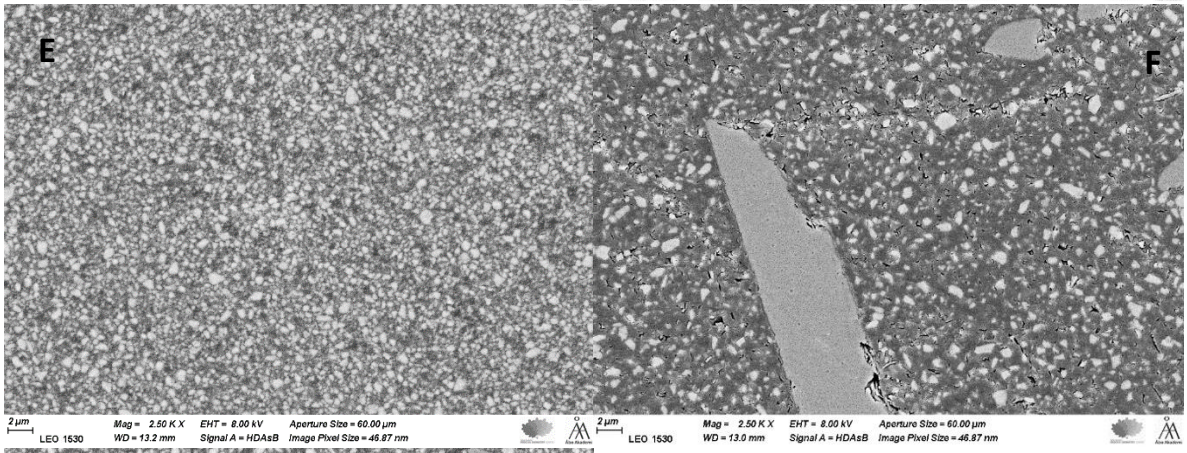
E
2 µm
LEO 1530
Mag = 2.50 K X
WD = 13.2 mm
EHT = 8.00 kV
Signal A = HDAsB
Aperture Size = 60.00 µm
Image Pixel Size = 46.87 nm

F
2 µm
LEO 1530
Mag = 2.50 K X
WD = 13.0 mm
EHT = 8.00 kV
Signal A = HDAsB
Aperture Size = 60.00 µm
Image Pixel Size = 46.87 nm

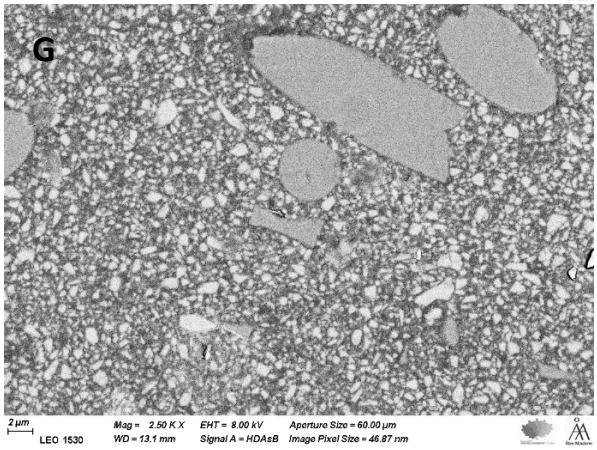
G
2 µm
LEO 1530
Mag = 2.50 K X
WD = 13.1 mm
EHT = 8.00 kV
Signal A = HDAsB
Aperture Size = 60.00 µm
Image Pixel Size = 46.87 nm

Figure 7. SEM photomicrographs of polished surface (4000 grit) of investigated materials (scale bar= 2 µm). (A) TEMP PRINT; (B) GR-17; (C) Essentia U; (D) Gradia Plus; (E) Cerasmart 270; (F) everX Flow; (G) SFRC Block.